Velocity-curvature dependence for chemical waves in the Belousov-Zhabotinsky reaction: Theoretical explanation of experimental observations

Pavel K. Brazhnik and John J. Tyson
Department of Biology, Virginia Polytechnic Institute and State University, Blacksburg, Virginia 24061
(Received 11 November 1998)

Experimental observations of V waves in the Belousov-Zhabotinsky reaction show a deviation from linearity of the front velocity dependence on curvature, which we seek to explain. The extent of deviations depends on the method of measuring velocity (V) and curvature (k). For one method, our theory predicts a cubic k-of-V curve, deviating from the eikonal approximation towards smaller V for large negative curvatures. This is shown to agree well with our numerical study of V waves in the Oregonator model and to be consistent with experimental results. [S1063-651X(99)03004-4]

PACS number(s): 82.40.Ck

The Belousov-Zhabotinsky (BZ) reaction provides an excellent experimental system for studying the geometry of dissipative traveling waves in reaction-diffusion systems. In bulk solution (usually gelled to prevent convection) and in thin layers of reagent, zones of oxidation are seen moving through a background of more reduced reagent. The moving front between reduced and oxidized zones is easily discerned, and its local curvature and velocity can be measured. The dependence of local front velocity V on curvature k gives much information about how the wave moves.

A theory of the effects of curvature on wave velocity was developed by Zykov [1] and by Tyson and Keener [2] using singular perturbation arguments. They proved, as is observed experimentally, that those parts of an excitation front with positive curvature in the direction of the movement propagate more slowly than those with negative curvature. The linear velocity-curvature dependence for slightly curved fronts,

$$V = V_0 - Dk, \tag{1}$$

(here V_0 is the velocity of a plane wave and D is diffusivity of the fast-changing component) is known as the eikonal approximation. It shows explicitly the stabilizing role of diffusion for such waves, and enables one to incorporate the curvature phenomenon into a coarse-scale geometrical model which has become a powerful tool in the study of waves in two and three dimensional (3D) excitable media (EM) [3–5]. Further theoretical exploration of the V-of-k dependence (analytical [1] and numerical [6]) has revealed its nonlinear character: while for negative curvature Eq. (1) is still believed to hold, for positive k it was shown to exhibit a critical value beyond which propagation of a continuous front is impossible.

Experimentally, the V-of-k dependence has been studied in the BZ reaction [7–10], aggregation patterns [11], and heart tissue [12]. All experiments confirm the linear dependence of V on k for modestly curved fronts. For larger positive curvatures, experiments are not able to establish the theoretically predicted deviation from Eq. (1) toward smaller V, but are consistent about the existence of a critical curvature.

Two experiments explore the V-of-k dependence for negative curvature in the BZ reaction. Almost a decade ago, from a study of cusps formed in the collision of two circular waves, the eikonal approximation (1) was pronounced to be valid far beyond the region of its applicability (if considered as a perturbation expansion) [7]. For very large curvatures though, the data obtained were, as mentioned by the authors, not reliable. The cusps monitored in such experiments are not stationary, they change their curvature and velocity with time, which was one of the major obstacles to obtaining reliable data. To eliminate this deficiency, the region of large negative curvatures was reexamined recently by making use of V-shaped waves [9,10], which are stationary propagating patterns and hence do not change their velocity and curvature with time. Surprisingly, for large negative curvatures, the data obtained indicate a strong deviation of V from Eq. (1) towards higher velocities, an observation that still remains unexplained.

In this paper we present a theoretical study of the velocity-curvature dependence for V waves based on an approximate partial differential equations (PDE) model. We explain deviations from the linear eikonal equation observed in experiments, and propose a nonlinear analytical expression for the V-of-k dependence which contains a parametric dependence on the angle α between the V wave's wings. The theory is shown to compare well with experiments on the BZ reaction and with numerical results for the Oregonator model.

$V(k)$ from V waves in BZ reaction. V waves are formed in the oblique collision of two plane waves—the colliding parts of the fronts annihilate, and after a corner between the plane waves becomes smooth, a stationary propagating wedge with finite negative curvature appears. The wedge travels as a stationary structure, without change of shape. Experimental studies of V waves in a regular liquid BZ and in the light sensitive version of BZ reaction in a silica gel were reported in [9,10]. In the former case a V-shaped silver wire was used to initiate patterns while in the latter case an initial pattern was generated by illuminating only a portion of the gel with some angle α. The pattern then quickly evolved in time to its final stationary configuration on which measurements were made. The authors have also performed a study of V-wave

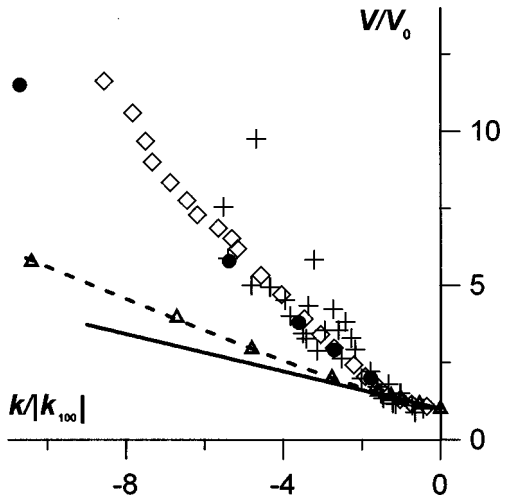

FIG. 1. Dependence of the normalized local front velocity V/V_0 versus the normalized front curvature $k/|k_{100}|$ (k_{100} is the curvature of the vertex of the V wave at $\alpha=100°$): diamonds correspond to numerical simulations with the two-variable Oregonator model [Eqs. (2a), (2b)], crosses are experimental data for measurements in the BZ reaction [9], and the solid line corresponds to the scaled eikonal equation $V/V_0=1-(1-V_{100}/V_0)(k/|k_{100}|)$. (The straight solid line assigned in Fig. 8 in [9] to the eikonal approximation does not have the correct slope, diamonds and crosses have to be interchanged in order to correspond to the description in the figure caption, and also the abscissa axis is $k/|k_{100}|$. These are corrected in [10] and in our Fig. 1. In our figure we have also omitted, in order to avoid cluttering, some experimental points from the original data set.) The triangles present our numerical data (values for parameters of the Oregonator model are as in [9], namely, $D=1.0$, $D_v=0$, $f=3.0$, $q=0.001$, $\varepsilon=0.01$) for the front defined as a constant-level line at the level $u_l=0.1$, and filled circles for $u_l=0.8$; space and time steps were $\Delta x=0.02$ and $\Delta t=0.0001$. The dashed line shows the corresponding curve resulting from our theory ($u_l=0.1$), Eq. (15), with $\beta=0.7$.

propagation numerically in a two-variable Oregonator model (see below). For each V wave with given α, the velocity of the wave as a whole was measured together with the curvature of the wave front at the vertex. Since for different angles α the velocity of the wave and its curvature at the wedge are different, the set of measurements for different α produces a function $V(k)$ reported in [9] and depicted in Fig. 1.

Analytical expression for $V(k)$. For theoretical calculations the BZ reaction is often modeled by the Oregonator, which describes only five of the most important reaction steps [13]. The Oregonator can be further simplified to a two-variable version written for the propagator variable u (dimensionless concentration of $HBrO_2$) and the recovery variable v (dimensionless concentration of ferriin) as [14]

$$\frac{\partial u}{\partial t}=\frac{1}{\varepsilon}\left(u-u^2-fv\,\frac{u-q}{u+q}\right)+D\Delta u(t,x,y), \tag{2a}$$

$$\frac{\partial v}{\partial t}=u-v+D_v\Delta v. \tag{2b}$$

Numerical values for the parameters in the above system usually are $D\sim1.0$, $D_v\sim0.5$, $f\sim1.0$, $q\sim0.001$, $\varepsilon\sim0.01$, and often diffusion of the recovery variable is neglected. ($D_v=0$ if the catalyst is immobilized in a gel [9].)

Consider stationary waves propagating along the X axis with velocity V_p (for plane waves $V_p=V_0$). For the traditional scaling used in Eqs. (2a) and (2b), the traveling front ($u\approx0$ carried to $u\approx1$) is narrow ($\Delta x\approx\varepsilon^{1/2}$) and moves rapidly ($V_p\approx\varepsilon^{-1/2}$). For our purposes, it is convenient to rescale time, $t'=t/\varepsilon$, and space, $x'=(\varepsilon D)^{-1/2}x$ and $y'=(\varepsilon D)^{-1/2}y$, to resolve the structure of the front ($\Delta x'\approx1$) and its velocity, $V_p'=(\varepsilon/D)^{1/2}V_p\approx1$. Now, in the moving frame, $\xi'=x'-V_p't'$, Eqs. (2a) and (2b) can be written (dropping the prime)

$$-V_pu_\xi=u(\xi,y)-u^2-fv\,\frac{u-q}{u+q}+u_{\xi\xi}+u_{yy}, \tag{3a}$$

$$-V_pv_\xi=\varepsilon(u-v). \tag{3b}$$

Analytical solutions for the system (3a),(3b) are not available even for one spatial dimension; therefore we proceed with further simplification. Similar to the way it was done in a singular perturbation approach [2], we distinguish the front, top, and tail parts of the excitation pulse, and because we are interested solely in solitary waves, we concentrate here only on the front part. For a fully developed excitation pulse, the value of v along the front of the solitary wave is small ($v\sim0.005$ for the set of parameters in Fig. 1) and changes slowly; therefore, we consider v to be in this region a constant ($v=v_0$). (We will not consider situations where the influence of the second component, v, on the front propagation is significant, e.g., the case of the lateral instability [15].) We are going to construct solutions for the problem (3a), (3b) which approximate the exact solution in the region of small u but are still large enough compared to q (e.g., $u\sim0.1$); therefore, for this purpose we set $(u-q)/(u+q)=1$ on the right hand side of Eq. (3a). Thus, for the lower part of the front of a propagating wave we end up with only one equation,

$$-V_pu_\xi=u-u^2-fv+u_{\xi\xi}+u_{yy}. \tag{4}$$

The latter can be reduced by the shift $u=u''+(1-\sqrt{1-4fv_0})/2$ and dilatation $u''=\sqrt{1-4fv_0}\tilde{u}$, $\tilde{\xi}=\sqrt{1-4fv_0}\xi$, $\tilde{y}=\sqrt{1-4fv_0}y$ to the 2D version of the well-known, quadratic Fisher equation

$$-c_pu_\xi=u-u^2+u_{\xi\xi}+u_{yy}, \tag{5}$$

where again we have omitted tildes. In Eq. (5), $c_p=V_p/(1-4fv_0)^{1/4}$.

In replacing Eqs. (2a),(2b) by Eq. (5), we are neglecting processes occurring behind the excitation front, the effect of which on the speed of a solitary wave is actually small. Equation (5) describes only a propagating front, because by fixing the inhibitor at small constant level we eliminate the mechanism which otherwise would prescribe a finite lifetime for the excitation. Since in the experiments we are going to discuss waves passing through the medium only once, it does not matter whether or not the medium regains excitability.

The V-shaped solution for the linearized version of Eq. (5) was constructed in [16]. It reads as

$$u(\xi,y)=\left\{M_1\exp\left[-\frac{c_0}{c_p}\xi\right]+M_2\exp\left[\left(-c_p+\frac{c_0}{c_p}\right)\xi\right]\right\}\cosh[\sigma^+\cos(\varphi_\infty)y], \tag{6}$$

where $M_{1,2}$ are some phase constants, c_0 is the plane front velocity for the Fisher traveling wave ($c_0\geqslant 2$), $\sigma^+=(-c_0+\sqrt{c_0^2-4})/2$, and φ_∞ is the asymptotic angle between each wing and the X axis ($\varphi_\infty=\alpha/2$). Also c_p, c_0, and φ_∞ are related to each other as

$$c_p=c_0/\sin(\varphi_\infty). \tag{7}$$

This is a special case of the local relationship

$$c_p=c/\sin(\varphi), \tag{8}$$

with c being the local normal velocity of the front, and φ being the angle between the tangent to the front line and the X axis ($\varphi|_{y\to\pm\infty}\to\pm\varphi_\infty$). For a constant level line, $u(\xi,y)=u_l\equiv$const, φ is defined by

$$\frac{dy}{d\xi}=-\left(\frac{u_\xi}{u_y}\right)_{u=u_l}=\tan(\varphi). \tag{9}$$

The curvature of the level line for the solution (6) can be evaluated via the standard formula $k=\{-d^2y/d\xi^2/[1+(dy/d\xi)^2]^{3/2}\}_{u=u_l}$. Combining then appropriately the last three expressions, one can find V as a function of k and u_l. If one accounts only for the leading term in ξ [the first term in Eq. (6)], this expression takes the form

$$k=-\sigma^+\sin^2\varphi_\infty\left(\frac{c}{c_0}\right)\left[1-\left(\frac{c}{c_0}\right)^2\right], \tag{10}$$

which does not depend on u_l. [An expression similar to Eq. (10) has been derived from an approximate V-shaped solution for the nonlinearized Fisher equation [16].]

In order to interpret this result, Eq. (10), in the context of the Oregonator model, we have to account for the rescaling we have done which introduces multiplicative prefactors to curvature and velocity,

$$k\to\frac{\sqrt{\varepsilon D}}{(1-4fv_0)^{1/4}}k,\quad c\to\frac{\sqrt{\varepsilon/D}}{(1-4fv_0)^{1/4}}V. \tag{11}$$

Also we want to recall here that the specific character of the dependence of σ^+ on c_0 is due to the linearization of the original equation [16]. In general, for the nonlinear case, this dependence is expected to be different. Therefore below we replace $-\sigma^+$ with some constant β whose value may depend on the dimensionless velocity of the plane excitation wave, $\tilde{V}_0$. For quantitative purpose we consider β as a free parameter of the order of unity (its value for the Fisher case). In fact, we will see later that $\beta=0.7$ fits our numerical data well. Thus Eq. (10) turns into

$$\frac{\sqrt{\varepsilon D}}{(1-4fv_0)^{1/4}}k=\beta\sin^2\varphi_\infty\left(\frac{V}{V_0}\right)\left[1-\left(\frac{V}{V_0}\right)^2\right]. \tag{12}$$

For small curvatures this cubic curve becomes

$$V=V_0-\frac{V_0\sqrt{\varepsilon D}}{2\beta(1-4fv_0)^{1/4}\sin^2\varphi_\infty}k \tag{13}$$

or, if we account for the rescaling (11),

$$V=V_0-\frac{\gamma D}{\sin^2\varphi_\infty}k. \tag{14}$$

The dimensionless constant $\gamma=\tilde{V}_0/2\beta(\tilde{V}_0)$ here would be 1 for the Fisher wave [when $\tilde{V}_0=(c_0)_{\min}$ and $\beta=-\sigma^+$]. Note that, in order to be consistent with our choice of small k, here we also have to replace $\sin^2\varphi_\infty$ by 1, since small curvatures can be achieved only for slightly curved V waves, for which $\varphi_\infty\sim\pi/2$. Finally, if we adopt that for EM γ differs negligibly from its value for the minimal Fisher wave, we recover for small k the eikonal approximation. For large negative curvature, on the other hand, Eq. (12) gives the deviation of V from the linear approximation towards smaller velocities.

In Eq. (14) we intentionally retained the $\sin^2\varphi_\infty$ factor to show explicitly that the slop in the eikonal approximation derived this way for V waves depends on the asymptotic angle of the V wave. In experiments, the angle was increasing for every new point $\{k(\varphi_\infty),V(\varphi_\infty)\}$, moving from zero to high negative curvatures, which, according to Eq. (14), introduces a larger slope for each point. The whole $V(k)$ curve obtained in this way obviously deviates monotonically from the linear dependence toward higher velocities. As a matter of fact, the experimental data were plotted with V in Fig. 1 as the velocity of the pattern as a whole, that is, V_p. The latter, as we know from Eq. (7), is defined in terms of the asymptotic angle. Accounting for this in Eq. (12) leads to

$$\frac{\sqrt{\varepsilon D}}{(1-4fv_0)^{1/4}}k=\beta\left(\frac{V_0}{V}-\frac{V}{V_0}\right), \tag{15}$$

which is the velocity-curvature relation to be compared to the kind of data reported in [9]. The curve (15) is depicted in Fig. 1 by a dashed line. It sketches correctly the nonlinear behavior demonstrated by the experimental data. The observed deviation is attributed, as discussed below, to different definitions of the front line in our theory and in [9].

The presence in Eq. (14) of a coefficient in front of k that depends on plane-wave velocity is consistent with another recent observation on curvature effects for excitation waves. Namely, a recent study [17] on wave trains in EM reported that not only does the first term in Eq. (1) depend on wave-train period, but also the second term has, apart from the diffusion coefficient, a train-period-dependent prefactor. But

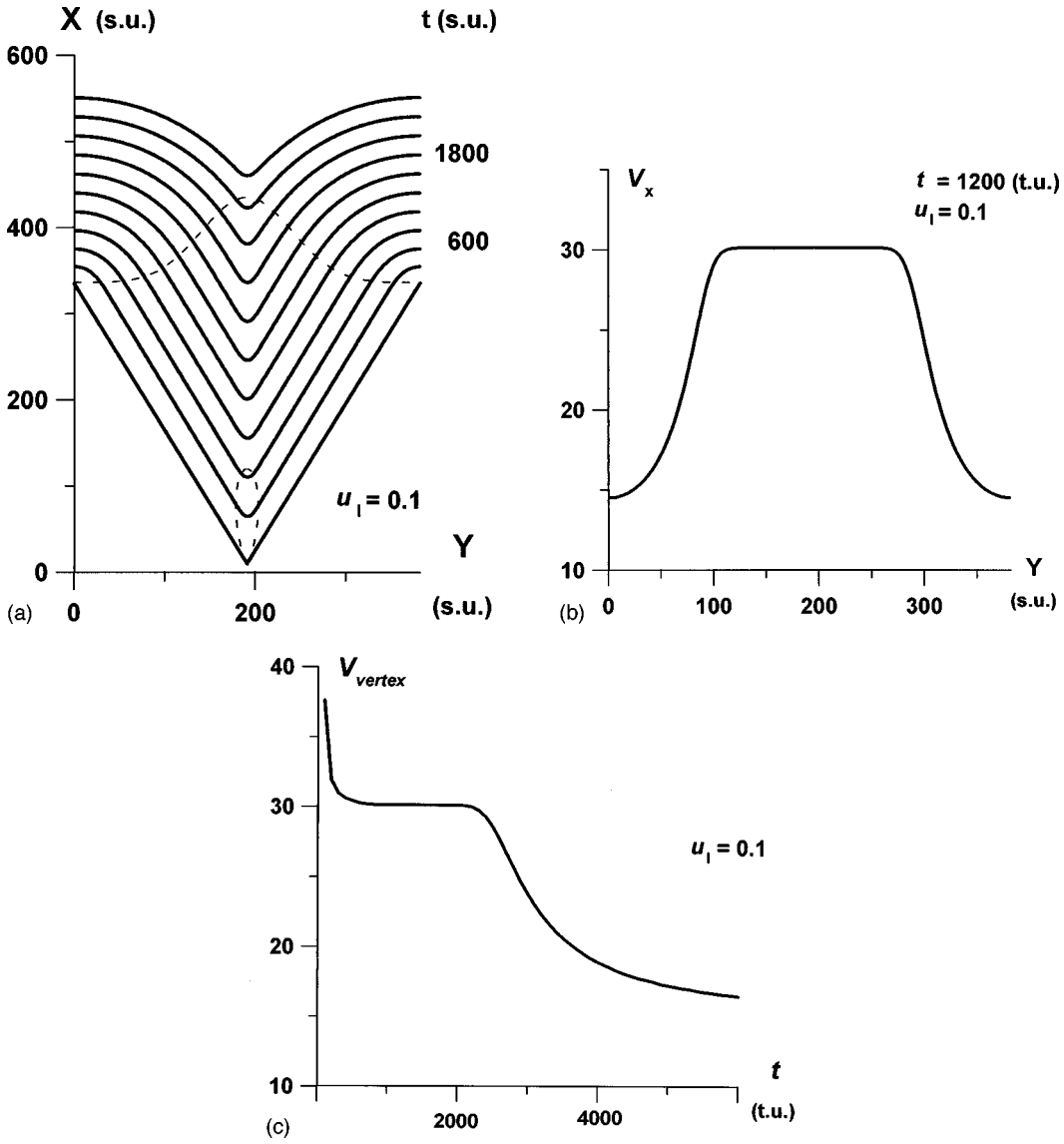

FIG. 2. Two plane waves collide at an angle $\alpha = 2\varphi_\infty = 60°$ in a stripe of width 382 space units (s.u.) and length 638 s.u., according to the numerical solution of the Oregonator equations (3a), (3b) for the parameters as in Fig. 1. (a) the V-shaped front propagating along the X axis in its positive direction is depicted in 11 different moments of time in the Cartesian frame of references; in the area between dashed lines the front propagates stationarily, without change of its shape; (b) the V_x component of the front velocity as a function of y; the plateau in the function $V_x(y)$ corresponds to the area where the vertex wave front propagates stationarily; and (c) the vertex velocity V_{vertex} as a function of time t; the plateau in the function $V_{\text{vertex}}(t)$ corresponds to the time when the vertex propagates stationarily.

wave-train period is connected to the front velocity by a dispersion relationship, and therefore the period dependence of the slope becomes equivalent to the velocity dependence of the slope.

Numerical results. In order to check our theory, we have performed a corresponding numerical study of V waves in system (2) in the region of parameters explored in [9]. Computations were performed on a sufficiently wide stripe. In order to produce V structures, we collide two plane waves, tilted (in opposite directions) to the long axis of the stripe (X axis) at angles $\pm\varphi_\infty/2$. No-flux boundary conditions were applied on each side of the stripe. As time proceeds, the initially sharp corner between the colliding waves smooths out. At the same time, the preboundary parts of the wave-front curve tend to become perpendicular to the boundary lines, as required by the no-flux boundary condition [see Fig. 2(a)]. The effect of these two processes on the rest of the front (areas between the vertex and preboundary layers) is different: while the negative curvature of the vertex k_{vertex} remains localized around the point of collision and quickly reaches its stationary value, the preboundary curvature disturbance propagates towards the vertex with velocity $U = V_0 \cot\varphi_\infty$ [9,18]. Thus if the width of the stripe W is such that the time needed for the preboundary perturbation to reach the vertex, $t^* = W/(2V_0 \cos\varphi_\infty)$, is much larger then the time for establishing the stationary curvature of the vertex, there exist unperturbed nearly straight regions on the wings of the wave connected by the stationary vertex, see Fig. 2(a). We do our measurements on this nearly stationary V wave before it disappears, when the perturbations from the boundaries approach the vertex area and convert the pattern into a plane wave. Figures 2(b) and 2(c) show that there is a

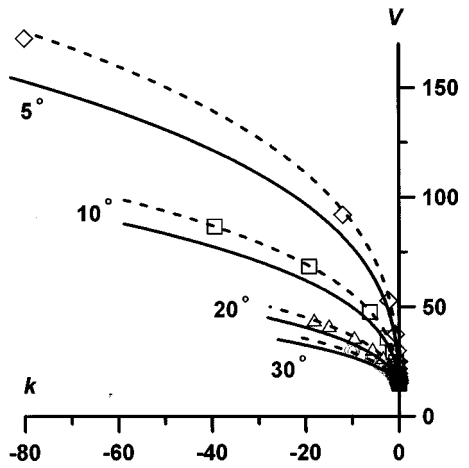

FIG. 3. The velocity-curvature dependence for V waves in the Oregonator model: open circles, triangles, squares, and diamonds are our numerical data for V waves with the angle between wings being 30°, 20°, 10°, and 5°, respectively (parameter values as in Fig. 1, $u_l=0.1$, and $t=1200$ time units); solid lines are corresponding analytical curves, Eq. (12), with $\beta=1$ as for the Fisher waves; and dashed lines are curves (12) but with $\beta=0.7$.

finite domain in space (y) and time when we can accurately measure V and k for a stationary V wave.

In our numerical experiments the width of the stripe was sufficiently large so that, when k_{vertex} is set to its stationary value, relatively large areas of the V-pattern wings remained unaffected by the preboundary perturbations. We have performed computations for V waves with different angles starting from $\alpha=10°$ up to $\alpha=120°$. Similarly to the way we did it in our theory, we defined the front line as a line of constant level and measured the curvature and the normal velocity along the front line, $k(y)$ and $V(y)$. These two together give a parametric (with the parameter y) representation of $V(k)$ for stationary V waves. As can be seen from Fig. 3, our theoretical curve turns out to be quite close to our measurements of $V(k)$ along the front of the stationary V wave. The agreement becomes even better if we choose in Eq. (12) $\beta=0.7$ instead of the Fisher wave value $\beta=1$.

We also collected numerical data about k_{vertex} and $V_{\text{vertex}}(\equiv V_p)$ for different angles α and therefore can construct a V-of-k curve equivalent to the one reported in [9,10] and shown in Fig. 1. Our numerical data are depicted in Fig. 1 by triangles and circles for low and high level cuts, $u_l=0.1$ and 0.8, respectively. The theoretical prediction for this kind of dependence, Eq. (15), which is valid only for low level cuts, is shown in Fig. 1 by a dashed line and agrees well with numerical results (triangles). Our numerical results indicate that the steepness of the $V_{\text{vertex}}(k_{\text{vertex}})$ curve depends on the level of the cut, which can be understood from the contour plot of the V wave shown in Fig. 4: level lines have essentially different curvature around the vertex—smaller for higher cuts—but since the pattern is stationary, all front lines must propagate with the same velocity. In [9,10] the front line was defined by the maxima at the wave front, therefore it is our numerical data for the high level cut (circles) which repeat pretty well the trend of numerical data from [9,10] (diamonds).

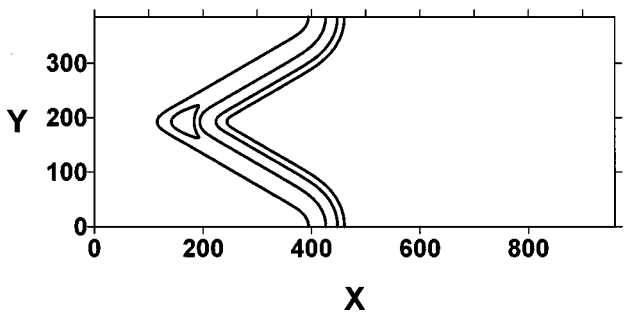

FIG. 4. The contour plot of the V-shaped wave with the angle between wings $\alpha=60°$ from our numerical experiment (parameters as in Fig. 1): only front lines are shown for the level cuts $u_l=0.1$ and $u_l=0.4$, while both front and back-front lines are shown for $u_l=0.8$ and $u_l=0.85$.

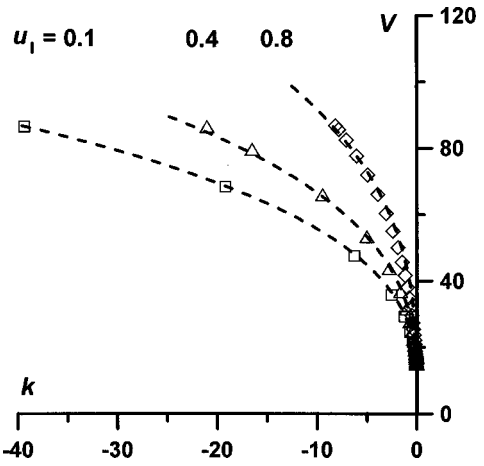

FIG. 5. Squares, triangles, and diamonds correspond to the velocity-curvature dependence for the V wave with $\alpha=10°$ numerically determined at the cut levels $u_l=0.1$, 0.4, and 0.8, respectively (the Oregonator model, parameters as in Fig. 1). Solid fitting curves are generated by our theoretical expression, Eq. (12) with adjusted β.

Numerical study of V waves allows us to investigate the effect of the cut level on the shape of the $V(k)$ curve. Figure 5 shows three $V(k)$ curves, numerically determined at the cut levels $u_l=0.1$, 0.4, and 0.8, for the V wave with $\alpha=10°$. As expected, the curves for higher cuts are ''lifted'' to higher velocities. Figure 5 shows, as well, that the dependence of $V(k)$ on cut level can be absorbed into the adjustable parameter β in our theoretical expression (12). The ''wedge'' of the V-k value observed in Fig. 5 represents a predicted confidence interval for experimental measurements of velocity and curvature. These measurements will be uncertain because the cut level (u_l) for a front is neither well defined nor easily reproducible. Nonetheless, theory predicts that measurements should be within this wedge, because $V(k)$ becomes independent of u_l for low cut levels ($u_l \leqslant 1$) and the front disappears if cut level is too high ($u_l > 1$).

Conclusions. In this work we have shown both analytically and numerically that the velocity-curvature relationship will deviate from linearity (the eikonal approximation), and that the extent of deviation depends on how the measurements are made. In experiments [9,10], $V(k)$ deviates to-

wards higher velocities for large negative curvatures, but our analytical result, Eq. (12), for stationary V waves, deviates in the opposite direction. We have shown that this discrepancy is due to different ways that $V(k)$ is measured in experiments and in our analysis. In experiments, a family of V waves is created, parametrized by α, the angle between the wings. Each V wave from this family generates one point on the $V(k)$ curve, given by the velocity $V_{\text{vertex}}(\alpha)$ and curvature $k_{\text{vertex}}(\alpha)$ of the vertex of the wave. In our analysis, from a single stationary V wave, we generate the entire $V(k)$ curve for $k \leqslant k_{\text{vertex}}$ by measuring local velocity $V(y)$ and curvature $k(y)$ of the front (parametrized by y, which increases from $y=0$ as we move away from the vertex). When we take into account precisely how the $V(k)$ dependence is measured, then our theory and reported experimental measurements are in good agreement.

We are grateful to V. Pérez-Muñuzury for supplying us with numerical and experimental data. This work was supported by NSF Grant No. CHE95-00763.

[1] V. S. Zykov, in *Simulation of Wave Processes in Excitable Media*, edited by A. T. Winfree (Manchester University Press, Manchester, 1987).
[2] J. P. Keener, SIAM J. Appl. Math. **46**, 1039 (1986); J. J. Tyson and J. P. Keener, Physica D **32**, 327 (1988).
[3] A. S. Mikhailov, *Foundations of Synergetics. I. Distributed Active Systems* (Springer-Verlag, Berlin, 1990).
[4] *Chemical Waves and Patterns*, edited by R. Kapral and K. Showalter (Kluwer, Dordrecht, 1995).
[5] A. S. Mikhailov and V. S. Zykov, Physica D **52**, 379 (1991); P. K. Brazhnik and J. J. Tyson, Phys. Rev. E **54**, 1958 (1996).
[6] J. Sneyd and A. Atri, Physica D **65**, 365 (1993); H. Ito, *ibid.* **79**, 16 (1994); C. Cobo *et al.*, Chaos Solitons Fractals **5**, 481 (1995); M. Courtemanche, *ibid.* **5**, 527 (1995).
[7] P. Foerster, S. Muller, and B. Hess, Science **241**, 685 (1988).
[8] P. Foerster, S. Muller, and B. Hess, Proc. Natl. Acad. Sci. USA **86**, 6831 (1989).
[9] V. Pérez-Muñuzuri *et al.*, Physica D **94**, 148 (1996).
[10] P. Brazhnik *et al.*, Chaos Solitions Fractals **10**, 99, (1999).
[11] P. Foerster, S. C. Muller, and B. Hess, Development (Cambridge, U.K.) **109**, 11 (1990).
[12] J. M. Davidenko *et al.*, Nature (London) **355**, 349 (1992).
[13] R. J. Field and R. M. Noyes, J. Chem. Phys. **60**, 1877 (1974).
[14] J. J. Tyson and P. C. Fife, J. Chem. Phys. **73**, 2224 (1980).
[15] A. F. M. Marée and A. V. Panfilov, Phys. Rev. Lett. **78**, 1819 (1997); S. C. Muller (private communication).
[16] P. K. Brazhnik and J. J. Tyson, SIAM J. Appl. Math. (to be published).
[17] A. P. Pertsov, M. Wellner, and J. Jalife, Phys. Rev. Lett. **78**, 2656 (1997).
[18] P. K. Brazhnik, Physica D **94**, 205 (1996).